

A New Algorithm for the Detection of Inter-cluster Galaxy Filaments using Galaxy Orientation Alignments

Kevin A. Pimbblet

Department of Physics, University of Queensland, Brisbane, 4072 Queensland, Australia
 pimbblet@physics.uq.edu.au

DRAFT: 14 NOVEMBER 2018 — DO NOT DISTRIBUTE

ABSTRACT

We present a new algorithm to detect inter-cluster galaxy filaments based upon the assumption that the orientations of constituent galaxies along such filaments are non-isotropic. We apply the algorithm to the 2dF Galaxy Redshift Survey catalogue and find that it readily detects many straight filaments between close cluster pairs. At large inter-cluster separations ($> 15h^{-1}$ Mpc), we find that the detection efficiency falls quickly, as it also does with more complex filament morphologies. We explore the underlying assumptions and suggest that it is only in the case of close cluster pairs that we can expect galaxy orientations to be significantly correlated with filament direction.

Key words: surveys – galaxies: clusters: general – large scale structure of Universe – cosmology: observations – methods: statistical

1 INTRODUCTION

Hierarchical structure formation models have long predicted that galaxy clusters grow through repeated mergers with other galaxy clusters and galaxy groups and continuous accretion of their surrounding matter (e.g. Zeldovich, Einasto & Shandarin 1982; Katz et al. 1996; Jenkins et al. 1998; Colberg et al. 2000; see also Bond, Kofman & Pogosyan 1996). Moreover, the accretion process usually happens in a very non-isotropic manner: galaxy filaments funnel matter onto large clusters along preferred directions (see Ebeling, Barrett & Donovan 2004; Kodama et al. 2001). Beyond the cluster core (say $>$ few virial radii), galaxy filaments are predicted (Colberg, Krughoff & Connolly 2004 and references therein) and observed to inter-connect many galaxy clusters in a complex, web-like manner (Pimbblet, Drinkwater & Hawkrigg 2004; Pimbblet & Drinkwater 2004; Dietrich et al. 2004; Gal & Lubin 2004; Ebeling, Barrett & Donovan 2004; Durret et al. 2003; Arnaud et al. 2000; Scharf et al. 2000; Kull & Bohringer 1999; Connolly et al. 1996 amongst others). It is this cosmic web that gives modern redshift surveys their striking & characteristic visual appearance (LCRS; 2dFGRS; SDSS) and quantifying the web's galaxy distribution and large-scale morphology has been a central focus of modern cosmology (e.g. Pandey & Bharadwaj 2004; Bharadwaj et al. 2004; Sheth 2004; Hikage et al. 2002; Hoyle et al. 2002; Tegmark et al. 2002; Connolly et al. 2002; Szapudi et al. 2002; Sahni et al. 1998; Shandarin & Yess 1998; Mecke, Buchert & Wagner 1994; Maddox et

al. 1990; Gott, Dickinson & Mellott 1986; Peebles & Groth 1975).

Filaments of galaxies (FOGs herein) are known to be highly important for the mass budget of the Universe (e.g. Colberg et al. 1999). Indeed, Cen & Ostriker (1999) show that for a Λ cold dark matter (Λ CDM) Universe, a large fraction, perhaps as much as half (Fukugita, Hogan & Peebles 1998), of baryonic material will not have been observed as it is situated in the inter-cluster media in a hot and tenuous gaseous phase. Along with the dark matter component and perhaps up to a quarter of the galaxian population, these baryons are preferentially situated in (inter-cluster) FOGs. Moreover, FOGs can provide tests of structure formation (cf. Colberg, Krughoff & Connolly 2004 with Pimbblet, Drinkwater & Hawkrigg 2004) and cluster evolution (see Colberg et al. 1999). Indeed, it is precisely in this low density filamentary regime that suppression of star-formation rates begins to occur (e.g. Balogh et al. 2004; Gomez et al. 2003; Lewis et al. 2002; see also Pimbblet 2003).

Finding FOGs is therefore becoming an important task in examining both structure formation theory and the evolution of stellar populations in galaxy clusters, yet there remains no good, single method to detect them. One method to find them was piloted by Briel & Henry (1995) who attempted to find evidence of the hot inter-cluster gas by searching for X-ray emission (from thermal bremsstrahlung) between galaxy clusters using *ROSAT* All-Sky Survey data. Although unsuccessful, the search yielded an X-ray surface brightness upper bound of 4×10^{-16} ergs cm⁻² s⁻¹ (0.5 –

2.0 keV) on any inter-cluster FOG present in their sample. Scharf et al. (2000) make a 5σ joint X-ray/optical detection of $> 12h_{50}^{-1}$ Mpc (0.5 deg) FOG with a surface brightness of 1.6×10^{-16} ergs cm $^{-2}$ s $^{-1}$. In the Shapley supercluster meanwhile, Kull & Bohringer (1999) find extended X-ray emission between a close cluster pair that is ~ 2.5 times brighter than Briel & Henry's (1995) bound, but this could be due to the clusters interacting with one another. The prospects of finding X-ray gas originating within filaments (at least at redshifts up to $z \sim 0.1$) is improving, however, due to the advent of satellites such as *XMM-Newton* (Pierre, Bryan & Gastaud 2000).

In the absence of X-ray data, other methods can also be used. Pimblet & Drinkwater (2004) find a significant overdensity of galaxies between the close clusters Abell 1079 and Abell 1084 by utilizing a statistical background correction technique. Both Dietrich et al. (2004) and Gray et al. (2002) analyze the region between close cluster pairs using weak gravitational lensing to infer the existence of inter-cluster FOGs. Spectroscopic observations also lead to concrete filamentary detections (e.g. Doroshkevich et al. 1996; Doroshkevich et al. 2001; Pimblet, Drinkwater & Hawkrigg 2004; Ebeling, Barrett & Donovan 2004; Pimblet, Edge & Couch 2005; see also Kodama et al. 2001 who employ photometric redshifts). In the case of less complex datasets (i.e. 2-dimensional with little or no colour information), FOGs can still be found by making use of techniques such as *Shapefinder* statistics (e.g. Bharadwaj et al. 2000; Pandey & Bharadwaj 2004); genus statistics (e.g. Hoyle et al. 2002; Hoyle, Vogeley & Gott 2002); minimal spanning trees (Doroshkevich et al. 2001); marked point processes (Stoica et al. 2005) and other multiscale approaches (e.g. Arias-Castro et al. 2004 and references therein).

This work presents a new algorithm to detect galaxy filaments in such low-complexity datasets by utilizing galaxy alignments. In section 2 we present the algorithm and the reasoning behind it. We evaluate our algorithm in section 3 by testing it on the 2dF Galaxy Redshift Survey (Colless et al. 2001). Our results are discussed in section 4 and we summarize our major conclusions in section 5.

2 THE ALGORITHM

The relative alignments and orientations of galaxies and clusters of galaxies has a long history. Binggeli (1982) and Struble (1990) find that the major axis of galaxy clusters are generally aligned exceptionally well with their first-ranked (usually a cD-type) galaxy and that close ($< 30h^{-1}$ Mpc) cluster pairs generally 'point to each other'; re-affirming the earlier work of Carter & Metcalfe (1980). Later work confirmed these results (e.g. West & Blakeslee 2000; Kitzbichler & Saurer 2003; Pereira & Kuhn 2004; see also Cabanela & Aldering 1998) and indicated that alignment effects between clusters can range up to tens of Mpc (e.g. Lambas et al. 1990; West 1994; Plionis 1994). Further, Fuller, West & Bridges (1999) find that the alignment effect between first-ranked galaxies and their host cluster, and between near cluster neighbours, is not restricted to only rich clusters, but also extends to much poorer clusters and galaxy groups as well.

Within clusters themselves, substructure is also found to align well with cluster orientation and with larger-scale fil-

aments that feed cluster's growth (Plionis & Basilakos 2002; West, Jones & Forman 1995; see also Plionis et al. 2003; Novikov et al. 1999; Kitzbichler & Saurer 2003). This scenario is (naturally) well-supported in Λ CDM hierarchical structure modelling (e.g. West, Villumsen, & Dekel 1991; van Haarlem & van de Weygaert 1993; West 1994; Bond, Kofman, & Pogosyan 1996; Dubinski 1998; Splinter et al. 1997; Tormen 1997; Hatton & Ninin 2001; Faltenbacher et al. 2002; Knebe et al. 2004; Hopkins, Bahcall & Bode 2005 amongst others) where filamentary structure funnels material along preferred directions toward clusters. If galaxy alignment does tend to follow the orientation of clusters and the filaments that feed them (and indeed their own galaxian neighbours; Mackey et al. 2002), then we can potentially make use of this fact in order to better detect and constrain the locations of inter-cluster FOGs. We note, however, that this assumption is unlikely to work in the case of very isolated clusters as violent relaxation will likely have eliminated any primordial alignments (Plionis et al. 2003; Coutts 1996; see also Quinn & Binney 1992; Lee 2004). Plionis et al. (2003) use this fact to distinguish between dynamically active, young and still accreting clusters (ones that have significant alignment between the cluster axis and constituent galaxies other than the first-ranked one) and inactive ones. Although Knebe et al. (2004) do not fully concur, they point out that filaments are indeed well-aligned with the halo that they feed.

Our algorithm broadly follows the procedure outlined by Plionis et al. (2003; see also Struble & Peebles 1985). Firstly, we select a (circular; square) region (with radius r ; of side l) of sky that is of interest to us (e.g. a region that contains a galaxy cluster) and extract from it all galaxies, N , with known position angles, θ_i ($1 \leq i \leq N$), relative to some cardinal vector (say East–West, for instance). The exact choice of which galaxies to use is explored in more detail in section 3.1. We then compare these angles to a proposed FOG angle, θ_f ($0 < \theta_f \leq 180$), again measured from the same cardinal direction:

$$\phi_{i,f} \equiv |\theta_i - \theta_f| \quad (1)$$

For an isotropic distribution, $\langle \phi_{i,f} \rangle \approx 45$ degrees. Hence, from the values of $\phi_{i,f}$ we can quantify the degree of anisotropy by following Struble & Peebles (1985):

$$\delta = \sum_i \frac{\phi_{i,f}}{N} - 45 \quad (2)$$

which has a standard deviation thus:

$$\sigma = \frac{90}{12N^{1/2}} \quad (3)$$

We interpret the resultant value of δ according to Table 1. Since our proposed filament angle, θ_f , may likely be wrong, we proceed to compute δ for the whole range of $0 < \theta_f \leq 180$ and find a value of θ_f that minimizes δ (i.e. we find the filament angle that aligns best with all θ_i in our particular region of sky; Table 1).

Assuming that there is a θ_f vector that minimizes δ , we can proceed in an iterative fashion by choosing a new region of sky in the direction indicated in order to trace out any (inter-cluster) FOG present.

Table 1. Interpretations of δ values.

Situation	Interpretation
$\delta \approx 0$	An isotropic distribution.
$\delta < 0$	Non-isotropic distribution. The galaxy angles align with the proposed filament angle.
$\delta > 0$	Non-isotropic distribution. The galaxy angles misalign with the proposed filament angle.

3 TESTING THE ALGORITHM

For convenience, we elect to test out our algorithm on the 2dFGRS catalogue (Colless et al. 2001) since it has already been searched visually for galaxy filaments by Pimbblet, Drinkwater & Hawkrigg (2004). The observations made by 2dFGRS are summarized by Colless et al. (2001) and here we only recount the pertinent detail. Briefly, the input catalogue for 2dFGRS is the APM survey of Maddox et al. (1990a,b). Targets for 2dF spectroscopy are selected^{*} to be brighter than an extinction-corrected magnitude limit of $b_J = 19.45$ within three strips of the APM survey (NGP, SGP and random fields) covering an area in excess of 1500 square degrees. Subsequently, quality (quality ≥ 3 ; see Colless et al. 2001) redshifts for 221414 galaxies have been published as part of the 2dFGRS FDR.

3.1 Biases

For 2dFGRS galaxies selected from the APM, one should expect that there would be no systematic bias with galaxy size. As found in a different sample by Plionis et al. (2003), galaxy size does become biased for smaller values of galaxy eccentricity. Figure 1 displays the relationship between isophotal galaxy size and eccentricity (as measured in the APM survey; see Maddox et al. 1990a for in depth descriptions of these quantities) for bright galaxies with $b_J < 19.0$ (some 3σ away from 2dFGRS's magnitude limit of $b_J = 19.45$; Pimbblet et al. 2001; Colless et al. 2001). At low values of isophotal area (< 400 pixels), there is a clear dip in the mean eccentricity. This bias is likely to be due to attempting to determine galaxy eccentricity from a limited, small number of pixels (see also Plionis et al. 2003). From herein, therefore, we only utilize galaxies with an isophotal area of greater than 400 pixels. This area is determined by making trial-and-error cuts in isophotal area and running the position angle test (described below) on the resultant galaxies. In order to use only galaxies that have distinct elongations, we also limit our selection to galaxies with an eccentricity > 0.05 .

Prior to examining 2dFGRS for filaments, it is also necessary to confirm that the position angles, θ_i , of galaxies within it are free from any contaminating biases. Figure 2 displays a histogram of position angles of all 2dFGRS galaxies. The distribution is approximately flat, containing no bin that is more than 1σ away from the expected mean value.

To better test for bias (or lack thereof) in these position angles, we utilize the Fourier transform of the position angles

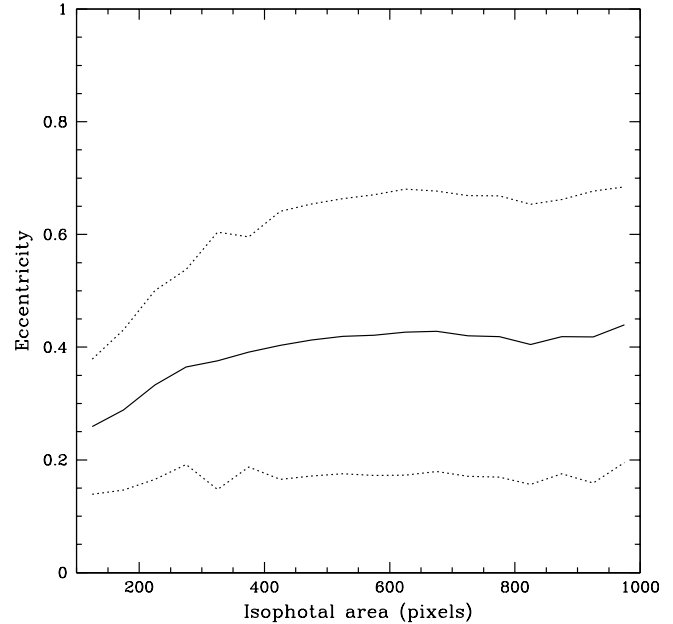


Figure 1. Galaxy eccentricity as a function of galaxy isophotal area for all galaxies with $b_J < 19.0$ in the NGP (the SGP follows a similar trend). The solid line denotes a running mean eccentricity and the dotted lines are 1σ errors on the mean. For galaxies with an isophotal area less than about 400 pixels, there is a systematic dip in eccentricity. Note that the plot is limited to galaxies with isophotal areas less than 1000 pixels. Beyond this range, the running mean remains near-constant about an eccentricity of approximately 0.43.

following the prescription of Struble & Peebles (1985; also see Plionis et al. 2003):

$$C_n = \left(\frac{2}{N}\right)^{1/2} \sum_{i=1}^N \cos 2n\theta_i \quad (4)$$

$$S_n = \left(\frac{2}{N}\right)^{1/2} \sum_{i=1}^N \sin 2n\theta_i \quad (5)$$

where the position angle θ_i runs from 1 to N and n is an integer ≥ 1 . Assuming that the position angles are randomly distributed, the average values of S_n and C_n should be zero with a standard deviation of 1, assuming $N \gg 1$ for a Gaussian distribution (Struble & Peebles 1985)[†]. The

^{*} The selection process does introduce some incompleteness (Pimbblet et al. 2001; Cross et al. 2004).

[†] The actual purpose of using the Fourier transforms is to examine if the galaxies have a particular preferred direction. To illumi-

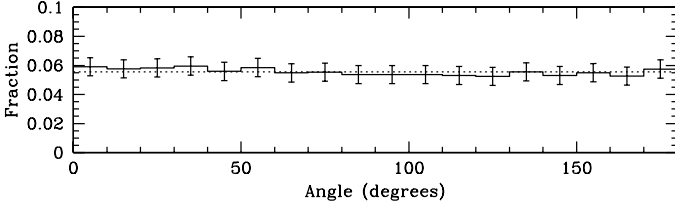


Figure 2. Histogram of the position angles, θ_i , of galaxies selected from 2dFGRS. Errorbars are simple Poissonian ones. A cursory inspection of this data suggests that the distribution of θ_i is approximately flat: all of the bins are within 1σ of the expected mean (denoted by the horizontal dotted line).

Table 2. Fourier transform of the distribution of position angles, θ_i . We consider that these values are consistent with isotropy.

n	C_n	S_n
1	2.6	-0.3
2	1.3	-1.3
3	0.6	-0.6
4	-0.9	0.5
5	-0.3	1.2
6	1.1	-1.3

fundamental and the first few harmonics for the sample is noted in Table 2. The individual values show no significant bias (i.e. a value $\gg 3$) and the distribution is consistent with a $N(0, 1)$ Gaussian under a standard KS test; thus we consider that these values are consistent with isotropy. Without the cut in galaxy isophotal area, these values are found to become significant indicating a distinct bias to a preferred direction(s).

3.2 Case study: Abell 1651

We start our evaluation by testing the algorithm on the (known) case of Abell 1651. Work by Pimblet, Drinkwater & Hawkrigg (2004) found that Abell 1651 is connected to Abell 1663 (a nearby cluster) by a Type I filament (i.e. a straight filament).

Firstly, we extract from 2dFGRS a region of galaxies contained within $r = 0.2$ degrees from the cluster centre of Abell 1651. Using these galaxies, we search for a correlation in direction by finding the angle θ_f that minimizes δ . We then repeat this process for a new region of sky in the direction indicated by the previous step (note that as this result shows two possible vectors, 180 degrees apart, we always choose the vector pointing closest to the next nearest cluster). The results of this analysis are displayed in Figures 3 and 4 which show the positions of the circular regions used and the values of δ against θ_f respectively.

Going from Abell 1651 to Abell 1663 is relatively easy:

nate this point, consider the C_1 component – a test for deviation from 90 and 180 degrees directions.

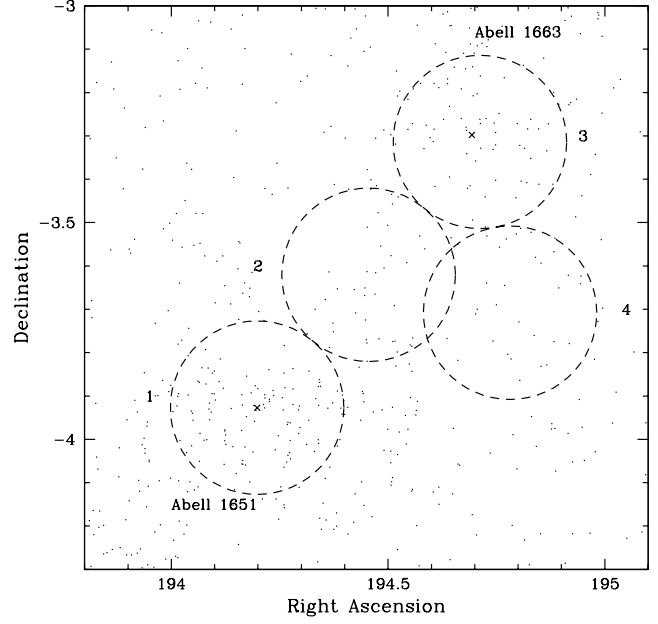


Figure 3. Area of 2dFGRS investigated. The crosses denote the approximate positions of Abell 1651 and Abell 1663 whilst the dashed circles are the positions of the $r = 0.2$ degree circular regions investigated using our algorithm. The numbers show the order in which the $r = 0.2$ circular regions are analyzed, starting at Abell 1651.

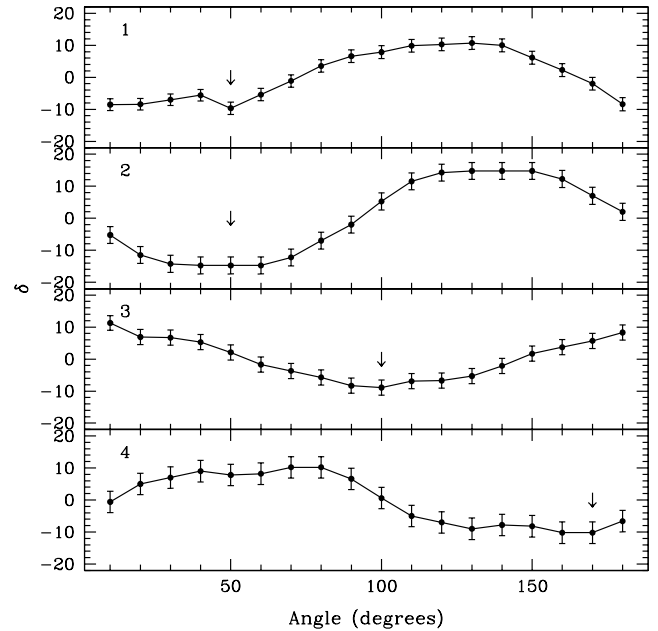


Figure 4. The δ values as a function of θ_f for each of the $r = 0.2$ degree circular regions identified from Figure 3. The downward pointing arrows show the minimum value of δ for each region. Errors are from equation (3).

the first two steps produce exactly the same result ($\delta_{min} = 50$ degrees), making for a very straight filamentary connection between the two clusters. In reverse, however, the clusters are still connected, but the connection becomes more curved. Step (3) (located nearly on top of Abell 1663) results in $\delta_{min} = 100$ degrees, which takes the path of the filament slightly away from the original straight one. This is likely due to contamination from galaxies on the opposite side of Abell 1663: taking only those galaxies in the semi-circle of step (3) closest to Abell 1651 would have yielded a position for step (4) that is much closer to step (2).

Nonetheless, the situation is rectified in the ‘real’ step (4) where $\delta_{min} = 170$ degrees. This shows that the next step would land the path back almost on top of step (2). Indeed, Pimblet, Drinkwater & Hawkrigg (2004; PDH) find that the connection between Abell 1651 and Abell 1663 is reasonably straight: a Type I filament in their nomenclature. This is certainly the case where one starts at Abell 1651. By starting at Abell 1663, however, would the resultant curvature have affected the (visual typing) result by PDH? In all likelihood, no. The distance of step (4) away from the inter-cluster axis is just less than about 0.4 degrees (Figure 3). At the mean redshift of the clusters ($z \approx 0.084$; Pimblet et al. 2001; Pimblet 2001) this separation equates to no more than 1.5 Mpc h_{100}^{-1} , i.e. very close to the inter-cluster axis and plenty smaller than the three-dimensional inter-cluster separation of ≈ 9 Mpc h_{100}^{-1} (PDH).

We note that even if the algorithm is able to find a filament between clusters A and B (by starting at cluster A), it does not necessarily follow that it will be able to find the same filament by starting at cluster B instead. This does not mean that the algorithm does not work. Both clusters A and B could be connected to multiple filaments. Indeed, the expected number of filaments connected to a given cluster scales well with the cluster mass (Colberg, Krughoff & Connolly 2004; PDH). The algorithm will preferentially find the neighbouring cluster or filament from whose direction the last clump of material fell in from. We also note that the algorithm will likely become confused if there is close alignment (i.e. superposition) of structures in the z direction.

3.3 Robustness

The 2dFGRS catalogue is known to be approximately 10 to 20 per cent incomplete at all magnitudes (Pimblet et al. 2001; Cross et al. 2004). The ‘missing galaxy’ population is not preferentially situated near cluster cores (Pimblet et al. 2001) and can therefore be simulated as a purely additional random galaxy sample that follows the clustering pattern and has random orientations, θ_i . Therefore to test if we can recover the filament signal in the presence of, what is essentially, increased noise, we repeat our experiment by adding in 15 per cent more galaxies in 100 Monte Carlo realizations.

The median value of δ_{min} out of the 100 realizations for steps (1) and (2) is then 50 ± 39 and 50 ± 14 degrees respectively. Since step (2) is directly inbetween the clusters, there is only a small amount of error on the median value. Step (1), however, is located at a cluster and the larger error on the average δ_{min} value is due to galaxies at the opposite end of the cluster to the filament, similar to what is seen at step (3), above. Indeed, the majority of the Monte Carlo realiza-

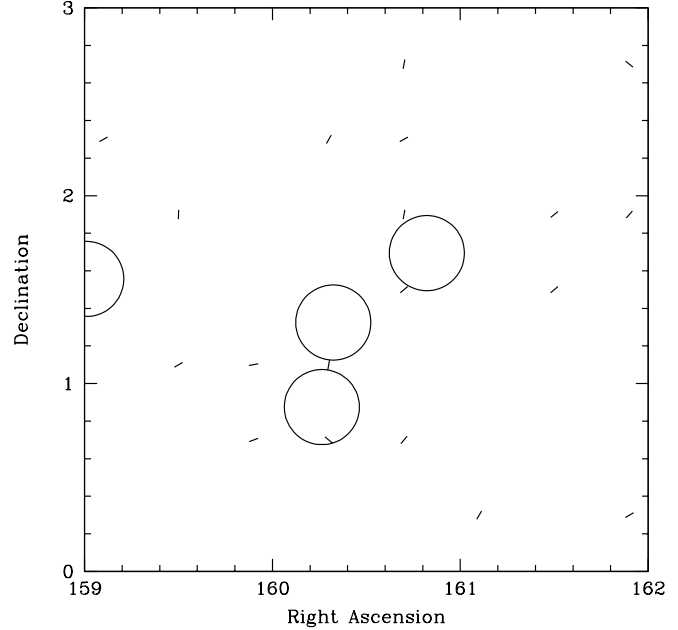


Figure 5. The algorithm as applied to the Leo-Sextans supercluster region of the NGP. Each line displays the vector corresponding to δ_{min} for each bin with a significant detection: $(\delta_{min}/\sigma) > 4.0$. The open circles denote the locations of known galaxy clusters taken from De Propris et al. (2002). Close cluster pairs display vectors pointing toward one another.

tions that do not result in $\delta_{min} = 50$ for step (1) generate $\delta_{min} = 180$. From Figure 4, it can be seen that $\delta = 180$ for step (1) is also a local minima. It is likely, therefore that Abell 1651 has multiple filaments or significant substructure (see Plionis & Basilakos 2002) falling in along the $\delta = 180$ vector.

4 DISCUSSION

To better examine any filaments present in 2dFGRS we now apply the algorithm to the entire NGP 2dFGRS dataset. This is accomplished by dividing the 2dFGRS NGP data up into squares of side $l = 0.2$ degrees and applying the algorithm to each square sequentially. Figure 5 displays the result of this in the region of the Leo-Sextans supercluster. Close cluster pairs, especially in regions of high cluster density (i.e. superclusters), display obvious (direct) inter-connections, but galaxy clusters at larger (say $>> 15h^{-1}$ Mpc or $>> \text{few degrees}$) separations seldom appear to do so.

Clearly the arbitrary choice of the centres of the $l = 0.2$ degree squares can affect our results significantly. Therefore, we repeat the analysis that we performed on Abell 1651 & Abell 1663 (see above) on other (close) cluster pairs identified previously by PDH. Comparing to PDH, we conclude that our algorithm has an efficiency of ~ 75 per cent at detecting filaments at inter-cluster separations of up to $15 h^{-1}$ Mpc. Morphologically, these filaments are mostly straight with some slightly curved ones (i.e. Type I and some Type II filaments; PDH). At larger inter-cluster separations, how-

ever, the detection efficiency rapidly decreases to zero for all filament types regardless of whether they are morphologically Type I or II.

Further, we find that other types of filament morphology such as ‘walls’ or, equally, ‘sheets’ (Type III filaments; PDH) do not display significantly cohesive galaxy orientations. This is borne out by re-analyzing the recent work of Pimblet, Edge & Couch (2005) who have discovered a large scale wall in the direction of Abell 22. We find that the galaxies belonging to their Type III filament do not display any preferred (global) galaxy orientation. We reach the same conclusion by re-analyzing the Type III and IV (‘clouds’) filaments found by PDH. With more irregular filaments (Type V; PDH), there are sometimes (~ 10 – 25 per cent of all bona-fide Type V filaments) significant galaxy orientations; particularly in the cases where galaxy clusters are joined by close multiple filaments. In highly irregular and lumpy Type V filaments, the orientations are statistically consistent with isotropy.

Why do only relatively straight and short inter-cluster filaments of galaxies possess significant non-isotropic distributions of galaxy orientation angles with respect to the filament in which they reside? Consider a brief thought experiment utilizing the laminar flow model (LFM) outlined by Kitzbichler & Saurer (2003; see also Aubert, Pichon & Colombi 2004). We know that filaments of galaxies can be thought of as funnels that direct material onto clusters (e.g. Plionis & Basilakos 2002; Knebe et al. 2004). In the direction that is perpendicular to the funnel’s direction (the infall direction), matter is generally becoming more dense and coalescing. Conversely, along the vector parallel to the infall direction matter will be elongated by tidal force.

Consider the case of a single, isolated, straight filament joining together two close galaxy clusters. The LFM succinctly suggests that the galaxies in the filament will elongate along the filament’s direction as they move to either end (i.e. the clusters) of the filament. If separated by a greater distance, those galaxies that start out near to the clusters will be the first ones to elongate significantly as time passes and the elongation will become more pronounced as they move closer to the gravitational potential of the cluster. Indeed, if the galaxies only move by up to $\sim 10h^{-1}$ Mpc since their creation (Coles, priv. comm.) it is little wonder that galaxies beyond $\gg 10h^{-1}$ Mpc from a cluster have had much chance to elongate and align with the filament, hence the longer the filaments (say, $\gg 15h^{-1}$ Mpc), the less likely they are to be detected by this method.

The situation is more complicated in the case of curved filaments. In general, the curving of such filaments is known to be toward a relatively far-removed tertiary mass (Pimblet, Drinkwater & Hawkrigg 2004; Colberg, Krughoff & Connolly 2004). The presence of such a tertiary mass (e.g. another cluster) would have the effect of ‘confusing’ the galaxy orientations; particularly of those that start out distant from the two primary clusters. With other filament morphologies (and indeed, branching of them), the gravitational attraction of the filament itself will become much more important, further mixing the position angles of constituent galaxies.

5 CONCLUSIONS

This work presents a new algorithm for detecting filaments of galaxies between clusters based upon the assumption that their constituent galaxies will possess orientations that are not isotropic in nature. Our major findings are as follows:

- The algorithm will preferentially find the filament from whose direction the last clump of material fell in from. This means that one may not recover the exact same filament between clusters A and B by starting at cluster A versus starting at cluster B.
- The algorithm works well on detecting the presence of straight Type I inter-cluster filaments of galaxies separated by short distances (up to $15 h^{-1}$ Mpc). Up to ~ 75 per cent of such filaments are easily recovered using this algorithm.
- Longer Type I and many Type II filaments do not display the same non-isotropic distribution of galaxy orientations that their shorter counterparts do.
- The orientations of galaxies belonging to Type III and IV inter-cluster galaxy filaments are statistically consistent with isotropy.
- We suggest that low detectability of long filaments and more irregular filaments can be explained by considering a basic laminar flow model: galaxies in straight, isolated filaments are more likely to become elongated toward the clusters that they connect than galaxies in filaments with more complex morphologies.

It would be interesting to investigate the star-formation rate along these filaments (say by using the η parameter suggested by 2dFGRS; see Madgwick et al. 2002) to see if galaxies that are aligned well with a filament have a vastly different value to those that are not (Plionis et al. 2003). It should also be the case that galaxies near the centre of filaments are much younger (more blue and spiral-like) than galaxies toward a terminus (i.e. a cluster).

This algorithm could also be used to find potential filaments that are hiding in the Zone of Avoidance (providing, of course, that individual galaxy ellipticities can be measured accurately there). For example, it would be a good, independent test of the suspected filament found by Kraan-Korteweg, Woudt & Henning (1997) connecting the Hydra and Antlia clusters. Lee (2004), however, cautions that on its own evidence favouring ‘coherent orientation of galaxies embedded in a sheet should not be taken as identical to the existence of the sheet itself’.

Lastly, we note that the issue of detecting FOGs in redshift surveys can also be thought of as a ‘join-the-dots’ type problem (Arias-Castro et al. 2004; see also Stoica et al. 2005). Using galaxy orientations would readily transform this into the vectorized problem of ‘join-the-darts’ (Arias-Castro et al. 2004) and it will be interesting to see, in the future, how the results of these algorithms compare to the one presented here.

ACKNOWLEDGMENTS

This work has benefitted enormously from conversations with participants attending the November 2004 Multiscale Geometric Analysis Workshop IV, held in Los Angeles and I wish to warmly thank Jean-Luc Starck for inviting me to participate.

I also want to express my gratitude to the referee, Jörg Colberg, for a prompt and useful report that has improved this work.

KAP was supported by an EPSA University of Queensland Research Fellowship and a UQRSF grant throughout the course of this work.

REFERENCES

- Arias-Castro E., Donoho D., Huo X., Tovey C., 2004, *Advances in Applied Probability*, submitted ([www-stat.stanford.edu / ~donoho / Reports / 2004 / CTD-Arias-etal.pdf](http://www-stat.stanford.edu/~donoho/Reports/2004/CTD-Arias-etal.pdf))
- Arnaud M., Maurogordato S., Slezak E., Rho J., 2000, *A&A*, 355, 461
- Aubert D., Pichon C., Colombi S., 2004, *MNRAS*, 352, 376
- Balogh M., et al., 2004, *MNRAS*, 348, 1355
- Bharadwaj S., Sahni V., Sathyaprakash B. S., Shandarin S. F., Yess C., 2000, *ApJ*, 528, 21
- Bharadwaj S., Bhavsar S. P., Sheth J. V., 2004, *ApJ*, 606, 25
- Binggeli B., 1982, *A&A*, 107, 338
- Bond J. R., Kofman L., Pogosyan, D., 1996, *Nature*, 380, 603
- Briel U. G., Henry J. P., 1995, *A&A*, 302, L9
- Cabanela J. E., Aldering G., 1998, *AJ*, 116, 1094
- Carter D., Metcalfe N., 1980, *MNRAS*, 191, 325
- Cen R., Ostriker J. P., 1999, *ApJ*, 514, 1
- Colberg J. M., White S. D. M., Jenkins A., Pearce F. R., 1999, *MNRAS*, 308, 593
- Colberg J. M., et al., 2000, *MNRAS*, 319, 209
- Colberg J. M., Krughoff K. S., Connolly A. J., 2004, *MNRAS in press* (astro-ph/0406665)
- Colless M., et al., 2001, *MNRAS*, 328, 1039
- Connolly A. J., Szalay A. S., Koo D., Romer A. K., Holden B., Nichol R. C., Miyaji T., 1996, *ApJ*, 473, L67
- Connolly A. J., et al., 2002, *ApJ*, 579, 42
- Coutts A., 1996, *MNRAS*, 278, 87
- Cross N. J. G., Driver S. P., Liske J., Lemon D. J., Peacock J. A., Cole S., Norberg P., Sutherland W. J., 2004, *MNRAS*, 349, 576
- De Propriis R., et al., 2002, *MNRAS*, 329, 87
- Dietrich J. P., Schneider P., Clowe D., Romano-Diaz E., Kerp J., 2004, preprint, astro-ph/0406541
- Doroshkevich A. G., Tucker D. L., Oemler A. J., Kirshner R. P., Lin H., Shethman S. A., Landy S. D., Fong R., 1996, *MNRAS*, 283, 1281
- Doroshkevich A. G., Tucker D. L., Fong R., Turchaninov V., Lin H., 2001, *MNRAS*, 322, 369
- Dubinski J., 1998, *ApJ*, 502, 141
- Durret F., Lima Neto G. B., Forman W., Churazov E., 2003, *A&A*, 403, L29
- Ebeling H., Barrett E., Donovan D., 2004, *ApJ*, 609, L49
- Faltenbacher A., Gottlöber S., Kerscher M., Müller V., 2002, *A&A*, 395, 1
- Fukugita M., Hogan C. J., Peebles P. J. E., 1998, *ApJ*, 503, 518
- Fuller T. M., West M. J., Bridges T. J., 1999, *ApJ*, 519, 22
- Gal R. R., Lubin L. M., 2004, *ApJ*, 607, L1
- Gómez P. L., et al., 2003, *ApJ*, 584, 210
- Gott J. R., Dickinson M., Melott A. L., 1986, *ApJ*, 306, 341
- Gray M. E., Taylor A. N., Meisenheimer K., Dye S., Wolf C., Thommes E., 2002, *ApJ*, 568, 141
- Hatton S., Ninin S., 2001, *MNRAS*, 322, 576
- Hikage C., et al., 2002, *PASJ*, 54, 707
- Hopkins P. F., Bahcall N., Bode P., 2005, *ApJ in press* (astro-ph/0409652)
- Hoyle F., et al., 2002, *ApJ*, 580, 663
- Hoyle F., Vogeley M. S., Gott J. R. I., 2002, *ApJ*, 570, 44
- Jenkins A., et al., 1998, *ApJ*, 499, 20
- Katz N., Weinberg D. H., Hernquist L., Miralda-Escude J., 1996, *ApJ*, 457, L57
- Kitzbichler M. G., Saurer W., 2003, *ApJ*, 590, L9
- Knebe A., Gill S. P. D., Gibson B. K., Lewis G. F., Ibata R. A., Dopita M. A., 2004, *ApJ*, 603, 7
- Kodama T., Smail I., Nakata F., Okamura S., Bower R. G., 2001, *ApJ*, 562, L9
- Kraan-Korteweg R. C., Woudt P. A., Henning P. A., 1997, *PASA*, 14, 15
- Kull A., Böhringer H., 1999, *A&A*, 341, 23
- Lambas D. G., Nicotra M., Muriel H., Ruiz L., 1990, *AJ*, 100, 1006
- Lee J., 2004, *ApJ*, 614, L1
- Lewis I., et al., 2002, *MNRAS*, 334, 673
- Mackey J., White M., Kamionkowski M., 2002, *MNRAS*, 332, 788
- Maddox S. J., Efstathiou G., Sutherland W. J., Loveday J., 1990a, *MNRAS*, 243, 692
- Maddox S. J., Efstathiou G., Sutherland W. J., 1990b, *MNRAS*, 246, 433
- Madgwick D. S., et al., 2002, *MNRAS*, 333, 133
- Mecke K. R., Buchert T., Wagner H., 1994, *A&A*, 288, 697
- Novikov D. I., Melott A. L., Wilhite B. C., Kaufman M., Burns J. O., Miller C. J., Batuski D. J., 1999, *MNRAS*, 304, L5
- Pandey B., Bharadwaj S., 2004, preprint, astro-ph/0409616
- Peebles P. J. E., Groth E. J., 1975, *ApJ*, 196, 1
- Pereira M. J., Kuhn J. R., preprint, astro-ph/0411710
- Pierre M., Bryan G., Gastaud R., 2000, *A&A*, 356, 403
- Pimblett K. A., 2001, Ph.D. Thesis (University of Durham)
- Pimblett K. A., Smail I., Edge A. C., Couch W. J., O'Hely E., Zabludoff A. I., 2001, *MNRAS*, 327, 588
- Pimblett K. A., 2003, *PASA*, 20, 294
- Pimblett K. A., Drinkwater M. J., 2004, *MNRAS*, 347, 137
- Pimblett K. A., Drinkwater M. J., Hawkrigg M. C., 2004, *MNRAS*, 354, L61 (PDH)
- Pimblett K. A., Edge A. C., Couch W. J., 2005, *MNRAS in press* (astro-ph/0412076)
- Plionis M., 1994, *ApJS*, 95, 401
- Plionis M., Basilakos S., 2002, *MNRAS*, 329, L47
- Plionis M., Benoist C., Maurogordato S., Ferrari C., Basilakos S., 2003, *ApJ*, 594, 144
- Quinn T., Binney J., 1992, *MNRAS*, 255, 729
- Sahni V., Sathyaprakash B. S., Shandarin S. F., 1998, *ApJ*, 495, L5
- Scharf C., Donahue M., Voit G. M., Rosati P., Postman M., 2000, *ApJ*, 528, L73
- Shandarin S. F., Yess C., 1998, *ApJ*, 505, 12
- Sheth J. V., 2004, *MNRAS*, 354, 332
- Splinter R. J., Melott A. L., Linn A. M., Buck C., Tinker J., 1997, *ApJ*, 479, 632
- Stoica R. S., Martinez V. J., Mateu J., Saar E., 2005, *A&A*, in press (astro-ph/0405370)
- Struble M. F., Peebles P. J. E., 1985, *AJ*, 90, 582
- Struble M. F., 1990, *AJ*, 99, 743
- Szapudi I., et al., 2002, *ApJ*, 570, 75
- Tegmark M., et al., 2002, *ApJ*, 571, 191
- Tormen G., 1997, *MNRAS*, 290, 411
- van Haarlem M., van de Weygaert R., 1993, *ApJ*, 418, 544
- West M. J., Villumsen J. V., Dekel A., 1991, *ApJ*, 369, 287
- West M. J., 1994, *MNRAS*, 268, 79
- West M. J., Jones C., Forman W., 1995, *ApJ*, 451, L5
- West M. J., Blakeslee J. P., 2000, *ApJ*, 543, L27
- Zeldovich I. B., Einasto J., Shandarin S. F., 1982, *Nature*, 300, 407